Thermal influences on optical properties of light-emitting diodes: a semiempirical model

Angel García-Botella, Antonio Alvarez Fernández-Balbuena, Daniel Vázquez-Moliní, and Eusebio Bernabeu

The application of LED technology to fields such as alphanumerical displays and traffic control is continuously increasing. Because the technology is used outdoors, it must be able to operate under various environmental conditions. Like all semiconductor devices, LED's have properties that change with temperature. We propose a semiempirical model, based on semiconductor solid-state theory, that predicts the changes in the emission spectrum including the effect of temperature changes on the optical properties of the LED, within a range appropriate for outdoor applications (0–40 °C). This model permits us to evaluate the changes in the output flux and the chromaticity coordinates of the LED. We checked this model with seven different LED's. © 2001 Optical Society of America

OCIS codes: 250.0250, 230.3670, 120.5630, 120.5240.

1. Introduction

LED's are becoming important components in many optical systems for outdoor applications. These components experience changes in the working temperature that are due to changes in the environmental conditions (season cycle or day cycle). These temperature changes produce different effects in the optical properties of the LED. The most common of these effects is decreasing output flux with increasing temperature, which typically follows an exponential law and is due to the increase in the phonon recombination probability. Another important variation in the optical properties is the change in the emission spectrum with temperature, which mainly consists of shifts and broadening.[1] This effect can produce significant changes in the output flux and in the chromaticity coordinates of the LED emission.

In this paper we evaluate the changes in the emission spectrum by means of a semiempirical model, based on semiconductor solid-state theory. We used this model to obtain a theoretical approximation for the experimental emission spectra of visible LED's, in a range of temperatures suitable for outdoor applications, between 0 and 40 °C. The model uses the Fermi function as carrier distribution function, a nonparabolic approximation for the density of states in the valence and conduction bands[2] and the Varshni empirical model for the variations of the gap energy E_g with temperature.[3] The model accurately predicts the changes in the emission spectrum that are due to the internal changes in the semiconductor with temperature.

2. Semiempirical Model

The spectral emission of the LED, $r(E)$, can be obtained by the convolution between the distribution of electrons in the conduction band, $n(E)$, and the distribution of holes in the valence band, $h(E)$, multiplied by the probability of spontaneous emission A_{12},[4]

$$r(E) = A_{12}[n(E)*h(E)], \tag{1}$$

where E is the energy and the asterisk denotes convolution.

The distribution functions for electrons and holes in the bands can be obtained by multiplication of the distribution function of carriers by the density of states in the band,

$$n(E) = N_n(E)F_n(E), \tag{2a}$$

$$h(E) = N_h(E)F_h(E), \tag{2b}$$

where $N_n(E)$ and $N_h(E)$ are the density of states for electrons and holes, respectively, and $F_n(E)$ and

The authors are with the Departamento de Óptica, Universidad Complutense de Madrid, Facultad de Ciencias Físicas, Ciudad Universitaria s/n, 28040 Madrid, Spain. A. García-Botella's e-mail address is angelgb@eucmos.sim.ucm.es.

Received 25 June 2000; revised manuscript received 10 October 2000.

0003-6935/01/040533-05$15.00/0

$F_h(E)$ are the distribution functions for electrons and holes, respectively. Electrons and holes as fermions are distributed in the bands following the Fermi function,

$$F_n = \frac{1}{\exp\left(\frac{E - E_{fn}}{kT}\right) + 1}, \tag{3a}$$

$$F_h = \frac{1}{\exp\left(\frac{E_{fh} - E}{kT}\right) + 1}, \tag{3b}$$

where E_{fn} and E_{fh} are the quasi-Fermi levels for electrons and holes in the LED under forward bias, k is the Boltzman constant, and T is the temperature.

The most common approximation for the density of states in the bands is the parabolic approximation, which assumes a perfect parabolic relation between the energy and the momentum. However, there are a number of studies that try to explain some physical phenomena in semiconductors with a nonparabolic approximation.[2,5,6] In our model we have chosen the nonparabolic approximation proposed by Smith and Brennan,[2] to make the model applicable to a wider range of LED's. This nonparabolic approximation is given by

$$xE^y = p^2/2m, \tag{4}$$

where x and y are the nonparabolic parameters, p is the momentum, and m is the mass of the carriers. Obviously, if $y = 1$, the nonparabolic relation becomes parabolic. For our purposes the x parameter acts as a multiplicative constant in the spectrum, so its value has no influence on the shape of the spectrum.

With this nonparabolic approximation we can deduce the density of states,[4] and we can obtain distributions for the electrons in the conduction band and for the holes in the valence band given by

$$n(E) = C_1(E - E_c)^{(3y/2)-1} \frac{1}{\exp\left(\frac{E - E_{fn}}{kT}\right) + 1}, \quad \text{for } E > E_c, \tag{5a}$$

$$h(E) = C_2(E_v - E)^{(3y/2)-1} \frac{1}{\exp\left(\frac{E_{fh} - E}{kT}\right) + 1}, \quad \text{for } E < E_v, \tag{5b}$$

where C_1 and C_2 are constants independent of the energy.

At this point we introduce the semiempirical relationship between the gap energy and the temperature, deduced by Varshni,[2]

$$E_g(T) = E_g(0) - \alpha T^2/(\beta + T), \tag{6}$$

where $E_g(0)$ is the extrapolated gap energy at 0 K and α and β are parameters that depend on the semiconductor. To maintain the top of the valence band at 0 energy, we introduced this expression in the distribution for electrons in the conduction band. Then the distributions for electrons and holes are given by

$$n(E) = C_1\left[E - E_g(0) + \frac{\alpha T^2}{\beta + T}\right]^{(3y/2)-1} \frac{1}{\exp\left(\frac{E - E_{fn}}{kT}\right) + 1}, \quad \text{for } E > E_g(T), \tag{7a}$$

$$h(E) = C_2(E_v - E)^{(3y/2)-1} \frac{1}{\exp\left(\frac{E_{fh} - E}{kT}\right) + 1}, \quad \text{for } E < E_v. \tag{7b}$$

The probability of spontaneous emission A_{12} depends on the energy in the form $A_{12} \propto E^2$,[4] but this dependence has only a small influence on the shape of the spectrum compared with the influence of Fermi exponential functions. Then, by convolving expressions (7a) and (7b) in Eq. (1), we can evaluate the emission spectrum for different LED's and test their reaction to temperature.

3. Experimental Setup

In our experimental setup we used surface-mounted LED's, approximately 2 mm high, 3 mm long, and 2 mm wide. These dimensions are small enough to allow for accurate measurements of the temperature in the LED chip. This temperature was measured with two Cr–Al thermocouples, in the two sides of the LED. The LED is placed in contact with a thermoelectric cooler, which permits us to control the temperature in the LED. The thermoelectric cooler is linked to a heat sink to achieve good pumping of heat by the thermoelectric cooler (Fig. 1).

We feed the LED with a voltage source; this provides a constant voltage in the LED, which ensures that the changes in the band structure are due only to the temperature changes.

The experimental procedure is the following: We feed the LED, at 25 °C, until we obtain the nominal current, 20 mA. At this point we cool the LED by means of the thermoelectric cooler, keeping the voltage constant, and then the current through the LED drops, owing to the rise in the energy gap (6). We cool the LED to 0 °C and measure the output spectrum with a spectrophotometer; we repeat the measurements at 20 and 40 °C, a range of temperatures suitable for outdoor applications (for example, in a hot climate).

4. Experimental Results

With the configuration shown in Section 3 (Fig. 1), we measured the spectrum of seven surface-mounted LED's from different companies, three of company A, three of company B, and one of company C, at three temperatures, 0, 20, and 40 °C.

Looking at the experimental and the semiempirical results (Fig. 2), we can verify that the LED emission

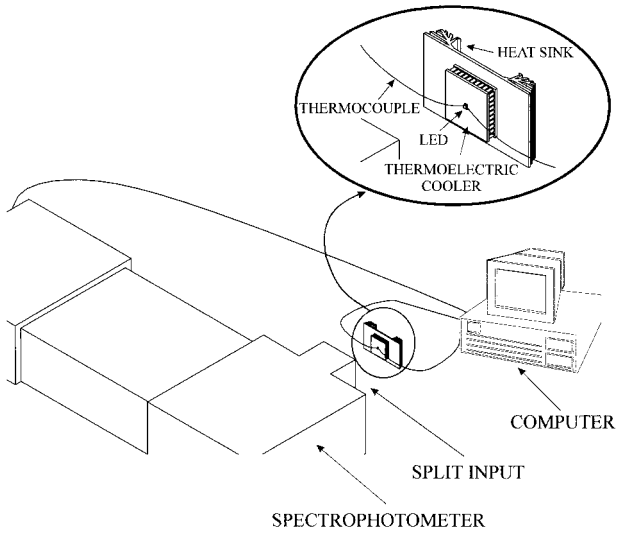

Fig. 1. Experimental setup used to measure LED spectrum and detail of LED cooling–heating system.

spectrum presents substantial changes that are due to temperature variations, not only in the peak wavelength but also in the spectral width.

In Fig. 2 we plot, as an example, the experimental and the semiempirical spectra for two LED's, 660-A of AlGaAs [Fig. 2(a)] and 585-C of GaAsP [Fig. 2(b)]. It can be seen that the semiempirical model accurately fits the experimental results for different kinds of spectra and that the spectra move and broaden with temperature. Table 1 shows the experimental and the semiempirical values for the shifts in the peak wavelength and the broadening of the spectrum that is due to temperature changes for all measured LED's and the semiconductor material for each LED. As can be seen, peak wavelength shifts as high as 11 nm and a bandwidth broadening of ~5 nm appear. The LED 595-A could not be measured at 40 °C, because it was damaged in its structure at that temperature. The estimated errors for these measurements are ±1 nm for peak wavelength measurements and ±0.8 nm for the bandwidth measurements.

Table 2 shows the parameters for the semiempirical model, $E_g(0)$, α, β, y, E_{fn}, and E_{fh}, which fit the experimental data. We treated the quasi-Fermi levels as being independent of temperature, since their variation in our temperature range is approximately $k\Delta T \approx 10^{-3}$ eV,[4] which is low compared with the values of quasi-Fermi levels obtained in the fitting. The only degenerate semiconductors are 625-A and 585-C, which have spectral bandwidths wider than 30 nm. It is also shown that a small value of α causes smaller shifts in the peak wavelength and that the deviations (y) from the parabolic approximation for the density of states are small.

Because of the spectral changes with temperature, there is a considerable influence in the photometric and the radiometric behavior of the LED's. We can evaluate the semiempirical and the experimental

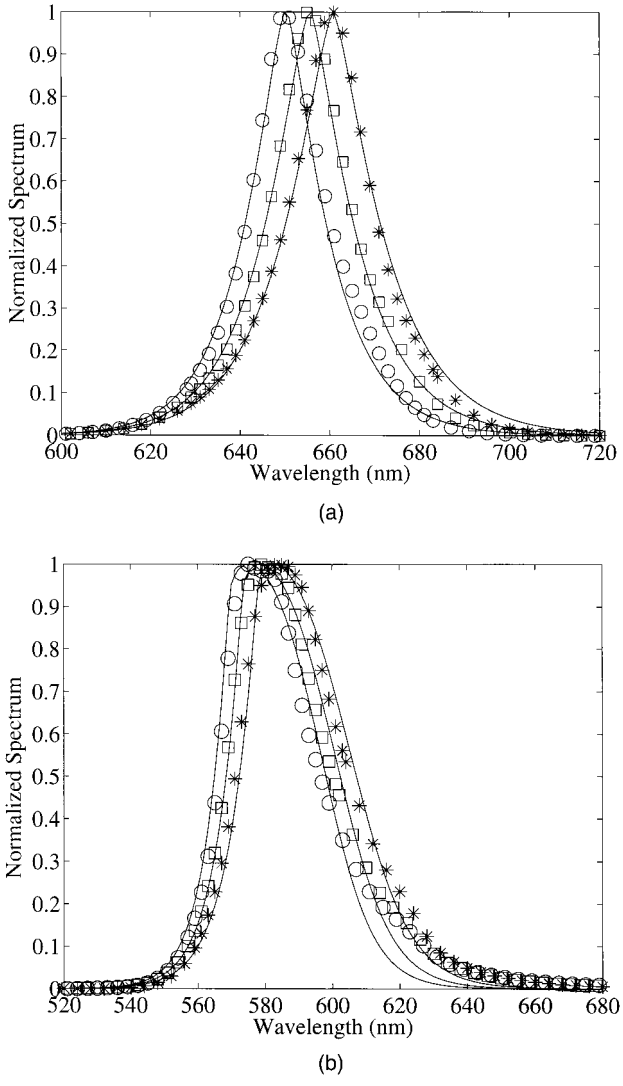

Fig. 2. Experimental spectra for two LED's at 0 (○), 20 (□), and 40 °C (∗). Solid curves correspond, for each case, to the semiempirical calculated results: (a) 660-A and (b) 585-C.

changes in the photometric and the radiometric fluxes by means of a simple integral,

$$\phi = \int_{-\infty}^{\infty} V(\lambda) S(\lambda) d\lambda, \tag{8}$$

where ϕ is the flux, $V(\lambda)$ is the photopic visibility curve if we are making photometric measurements or is equal to 1 for radiometric measurements, and $S(\lambda)$ can be the semiempirical or the experimental spectrum of the LED.

Table 3 shows the experimental and the semiempirical results of the variation with temperature of radiometric flux, in arbitrary units for all the LED's. These values are relative only to the shape of the spectrum and do not take into account the quantum efficiency of the LED. The variation goes from 6.5% in the smallest case (585-C) to more than 20% for the highest one (630-B). It is also shown that the semiempirical results are within the error range of

Table 1. Experimental (E) and Semiempirical (S) Values of Peak Wavelengths (λ_p) and Spectrum Bandwidth ($\Delta\lambda_{1/2}$) for all Measured LED's

		Temperature (°C)					
		0		20		40	
		λ_p (nm)	$\Delta\lambda_{1/2}$ (nm)	λ_p (nm)	$\Delta\lambda_{1/2}$ (nm)	λ_p (nm)	$\Delta\lambda_{1/2}$ (nm)
595-A	E	591	18.5	594	19.5		
(InGaAlP)	S	590.5	17.8	594	19.2		
625-A	E	622	33.6	624	36	626	38.8
(GaAsP)	S	622	35	624	36.3	626	37.6
660-A	E	650	19	656	20	661	21
(GaAlAs)	S	650	18.1	656	19.8	661	21.2
592-B	E	589	13.2	593.5	14.6	598	15.6
(InGaAlP)	S	589.5	13.2	593.5	14.4	598	15.7
609-B	E	609	13.2	614	14.5	618	16.3
(InGaAlP)	S	609	12.9	612.5	14.5	616.5	15.9
630-B	E	632	14	636.5	16	641	18.5
(InGaAlP)	S	632	14.7	636.5	16.1	641	17.7
585-C	E	575	30.8	578	32	586	34
(GaAsP)	S	575	33.2	579	33.9	582.5	34.8

Table 2. Estimated Parameters for the Semiempirical Model That Fit the Experimental Measurements

λ_p (nm)	$E_g(0)$(eV)	(10^{-4} eV K^{-1})	β (K)	y	E_{fn} (eV)	E_{fh} (eV)
595-A	2.22	7.15	175	1.04	1	0.32
625-A	2.11	5.1	151	0.94	1.07	−0.1
660-A	2.07	8.3	107	0.9	1	0.1
592-B	2.24	8	157	0.82	0.84	0.6
609-B	2.14	8	310	0.79	0.7	0.21
630-B	2.08	8.6	196	0.81	0.65	0.22
585-C	2.33	9	175	1.02	0.58	−0.1

the experimental ones. However, Table 4 shows the experimental and the semiempirical results for the variation with temperature of the photometric flux, relative to the shape of spectrum, in arbitrary units. This table shows that the photometric flux does not present significant changes with temperature, because of the effect of the $V(\lambda)$ function; with the increase in T the peak wavelength of the spectrum shifts to greater wavelengths where $V(\lambda)$ is lower. This loss in photometric flux is compensated with the broadening of the spectrum with T, so the photometric flux remains practically invariable. However,

Table 3. Semiempirical and Experimental Radiometric Fluxes, Relative to Spectrum Shape in Arbitrary Units, for all LED's

	Semiempirical (and Experimental) Radiometric Fluxes Temperature (°C)		
λ_p	0	20	40
595-A	21.9 (21.1 ± 0.5)	23.7 (23 ± 0.5)	
625-A	38.9 (39.5 ± 1)	41 (42.3 ± 1)	43.5 (45.1 ± 1)
660-A	23.2 (23.2 ± 0.6)	25.2 (25.2 ± 0.6)	27.1 (26.5 ± 0.6)
592-B	17.4 (17.4 ± 0.4)	18.9 (18.8 ± 0.4)	20.4 (20.6 ± 0.5)
609-B	17.1 (16.9 ± 0.4)	18.9 (18.9 ± 0.4)	20.5 (20.9 ± 0.5)
630-B	19.3 (18.9 ± 0.5)	21.2 (20.8 ± 0.5)	23 (23.7 ± 0.6)
585-C	35.9 (37.8 ± 0.9)	37 (38.6 ± 0.9)	38.3 (39.86 ± 1)

Table 4. Semiempirical and Experimental Photometric Fluxes, Relative to Spectrum Shape in Arbitrary Units, for all LED's

	Semiempirical (and Experimental) Photometric Fluxes Temperature (°C)		
λ_p	0	20	40
595-A	16 (15.7 ± 0.4)	16.3 (16.2 ± 0.4)	
625-A	12.9 (12.8 ± 0.3)	12.5 (12.4 ± 0.3)	11.9 (11.8 ± 0.3)
660-A	2.81 (2.77 ± 0.07)	2.46 (2.39 ± 0.07)	2.12 (2.12 ± 0.07)
592-B	13.3 (13.2 ± 0.3)	13.7 (13.7 ± 0.3)	13.7 (14.0 ± 0.3)
609-B	9.1 (8.9 ± 0.2)	9.1 (9.2 ± 0.2)	9 (9.4 ± 0.2)
630-B	5.19 (5.06 ± 0.12)	4.8 (4.97 ± 0.12)	4.4 (4.84 ± 0.12)
585-C	29.5 (29 ± 0.7)	28.9 (28.9 ± 0.7)	28 (28.5 ± 0.7)

Table 5. Semiempirical CIE[a] 1931 Chromatic Coordinates for All LED's

	x (Temp. in °C)			y (Temp. in °C)		
λ_p	0	20	40	0	20	40
595-A	0.573	0.589		0.426	0.410	
625-A	0.680	0.681	0.682	0.319	0.318	0.318
660-A	0.718	0.720	0.721	0.282	0.280	0.279
592-B	0.567	0.586	0.604	0.432	0.413	0.395
609-B	0.651	0.660	0.669	0.348	0.339	0.330
630-B	0.700	0.704	0.708	0.299	0.295	0.292
585-C	0.520	0.541	0.562	0.479	0.458	0.437

[a]CIE, Commission Internationale de l'Eclairage.

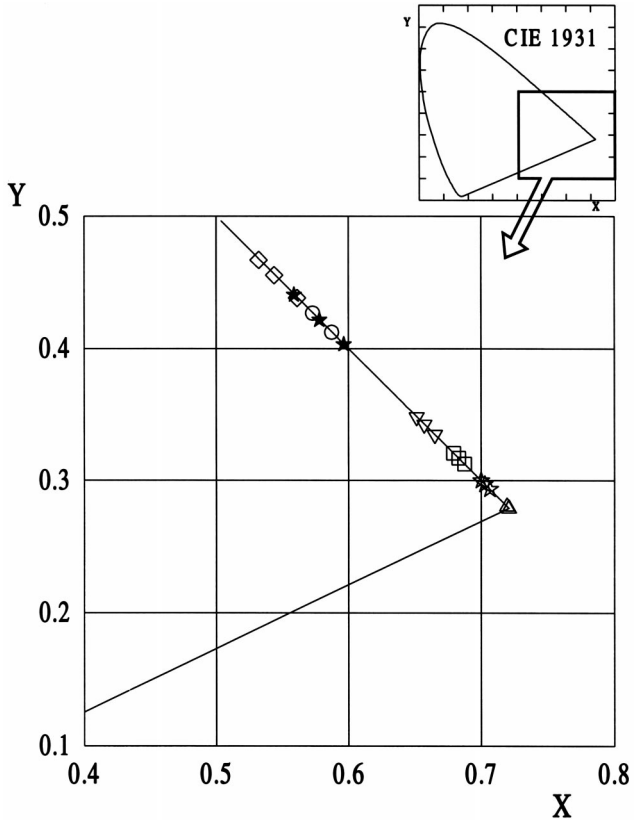

Fig. 3. Semiempirical variations of the CIE 31 (Commission Internationale de l'Eclairage) chromatic coordinates for all LED's: (◇) company C $\lambda_{peak} = 585$, (★) company B $\lambda_{peak} = 592$, (○) company A $\lambda_{peak} = 595$, (▽) company B $\lambda_{peak} = 609$, (□) company A $\lambda_{peak} = 625$, (☆) company B $\lambda_{peak} = 630$, and (△) company A $\lambda_{peak} = 660$.

the LED emission presents a significant variation in the chromatic coordinates, which produces variations in the specifications of optical systems that use these elements. These variations are shown in Table 5 and in Fig. 3.

5. Conclusions

In this paper we have studied the effect of temperature in the spectrum of LED's, for a range suitable for outdoor applications, between 0 and 40 °C. We have proposed a semiempirical model based on solid-state theory, which includes a nonparabolic approximation for the density of state and the Varshni relation for the gap dependence on temperature. The model predicts accurately the shape of the emission spectrum and its changes with the temperature. It has been checked experimentally, obtaining good agreement for different LED's. This temperature effect produces changes in the optical properties of LED's that can be well evaluated with the semiempirical model. The output radiometric flux can change more than 20% in this temperature range. The output photometric flux does not change significantly, owing to the shape of $V(\lambda)$ function, but significant changes in the chromatic coordinates of the LED appear. Then for human vision it is not necessary to adapt the LED radiance, but it will be necessary to take into account these colorimetric changes when they are important, e.g., if LED's are used in traffic signals for which chromatic requirements are restrictive.

The authors thank A. Gonzalez-Cano for his suggestions. This research was supported by Proyecto para el Estímulo a la Transferencia de Resultados de Investigación (PETRI) grant 95-0344-OP, a project of the Comisión Interministerial de Ciencia y Tecnología of Spain.

References

1. T. S. Moss and M. Balkanski, *Handbook on Semiconductors: Optical Properties of Semiconductors* (Elsevier Science, Amsterdam, 1994), Vol. 2.
2. A. W. Smith and K. F. Brennan, "Non-parabolic hydrodynamics formulations for the simulation of inhomogeneous semiconductor devices," Solid-State Electron. **39,** 1659–1668 (1996).
3. I. A. Vainshetein, A. F. Zatsepin, and V. S. Kortov, "Applicability of the empirical Varshni relation for the temperature dependence of the width of the band gap," Phys. Solid State **41,** 905–908 (1999).
4. K. J. Ebeling, *Integrated Optoelectronics* (Springer-Verlag, Berlin, 1993).
5. A. W. Smith and K. F. Brennan, "Comparison of non-parabolic hydrodynamic simulations for semiconductor devices," Solid-State Electron. **39,** 1055–1063 (1996).
6. M. C. Cheng, L. Guo, R. M. Fithen, and Y. Luo, "A study of the non-parabolic hydrodynamic modelling of a sub-micrometre n^+–n–n^+ device," J. Phys. D **30,** 2343–2353 (1997).